An oxo-ferryl tryptophan radical catalytic intermediate in cytochrome *c* and quinol oxidases trapped by microsecond freeze-hyperquenching (MHQ)

Frank G.M. Wiertz[a], Oliver-Matthias H. Richter[b], Alexey V. Cherepanov[a], Fraser MacMillan[c], Bernd Ludwig[b], Simon de Vries[a,*]

[a]*Department of Biotechnology, Delft University of Technology, Julianalaan 67, 2628 BC, Delft, The Netherlands*
[b]*Biozentrum, Molecular Genetics, J.W. Goethe-Universität, Marie-Curie-Str. 9-11, D-60439 Frankfurt am Main, Germany*
[c]*Institut für Physikalische and Theoretische Chemie and Center for Biomolecular Magnetic Resonance, J.W. Goethe-Universität, Marie-Curie-Str. 9-11, D-60439 Frankfurt am Main, Germany*

Received 24 July 2004; revised 17 August 2004; accepted 17 August 2004

Available online 11 September 2004

Edited by Stuart Ferguson

Abstract The pre-steady state reaction kinetics of the reduction of molecular oxygen catalyzed by fully reduced cytochrome oxidase from *Escherichia coli* and *Paracoccus denitrificans* were studied using the newly developed microsecond freeze-hyperquenching mixing-and-sampling technique. Reaction samples are prepared 60 and 200 μs after direct mixing of dioxygen with enzyme. Analysis of the reaction samples by low temperature UV–Vis spectroscopy indicates that both enzymes are trapped in the P_M state. EPR spectroscopy revealed the formation of a mixture of two radicals in both enzymes. Based on its apparent *g*-value and lineshape, one of these radicals is assigned to a weakly magnetically coupled oxo-ferryl tryptophan cation radical. Implications for the catalytic mechanism of cytochrome oxidases are discussed.

Keywords: Cytochrome oxidase; Microsecond freeze-hyperquenching; Tryptophan radical transient kinetics; Biocatalysis; Bioenergetics

1. Introduction

Cytochrome oxidases couple dioxygen reduction to proton translocation to generate a proton electrochemical gradient, for e.g., ATP production. Physiologically, these enzymes act as terminal electron acceptors and are found in Archaea, Bacteria and Eucarya [1–3]. The overall reaction for cytochrome oxidases from the heme–copper oxidase superfamily such as cytochrome *c* oxidases (i.e., cytochrome aa_3 from *Paracoccus denitrificans*) or quinol oxidases (i.e., cytochrome bo_3 from *E. coli*) proceeds according to [4]:

$$4\mathrm{cyt}\,c^{2+}/2\mathrm{QH_2} + \mathrm{O_2} + 8\mathrm{H_C^+} \rightarrow 4\mathrm{cyt}\,c^{3+}/(2\mathrm{Q} + 4\mathrm{H_P^+}) + 2\mathrm{H_2O} + 4\mathrm{H_P^+}$$

where "C" and "P" denote the cytoplasmic and the periplasmic space of the bacterial cell.

The catalytic mechanism of oxidases has been studied extensively over a long period of time with a great number of different techniques [5–12], which has led to a detailed understanding of the catalytic mechanism [13–16]. Accordingly, cleavage of the O–O bond had been proposed to involve Trp or Tyr residues from the enzyme [5]; later, H-atom donation by Y280 (*P. denitrificans* numbering system) was postulated, a residue covalently linked to a histidine (H276) ligating Cu_B. Indeed, a neutral tyrosine radical has been detected using the iodine labeling technique in bovine cytochrome aa_3 oxidase prepared in the P_M state [10]. In *P. denitrificans* cytochrome aa_3 oxidase treated with stoichiometric amounts of H_2O_2, a tyrosine radical was also detected by EPR [17,18], which has recently been identified as Y167, a residue close to the active site [18,19].

Other studies on the bovine cytochrome *c* oxidase employing excess H_2O_2 [20,21] suggest the formation of a porphyrin cation radical and/or a tryptophan cation radical. In all these aforementioned studies, the radicals were formed under quasi-equilibrium conditions hampering conclusions on their role in the catalytic mechanism. To overcome this problem, a novel pre-steady state kinetic method to analyze chemical reactions has recently been developed in our laboratory. The microsecond freeze-hyperquenching device (MHQ) enables chemical reaction intermediates to be trapped within 140 μs [12]. Studies on the reduction of molecular oxygen catalyzed by cytochrome bo_3 oxidase from *E. coli* showed the formation of a transient radical; unfortunately, the low enzyme concentration used in EPR studies necessitated saturating power for measurements preventing determination of its nature [12]. The MHQ setup has now been modified employing a rotating cold plate instead of cold iso-pentane to quench the reaction, yielding quench times of 60 μs and more concentrated EPR samples. Using the cold plate MHQ setup, we have studied the direct oxidation by O_2 of cytochrome aa_3 oxidase from *P. denitrificans* and cytochrome bo_3 oxidase from *E. coli*. The kinetic studies reported here indicate the formation of two radical species in the P_M state. One of these is assigned to an oxo-ferryl coupled tryptophan cation radical.

* Corresponding author. Fax: +31-15-278-2355.
E-mail address: s.devries@tnw.tudelft.nl (S. de Vries).

0014-5793/$22.00
doi:10.1016/j.febslet.2004.08.048

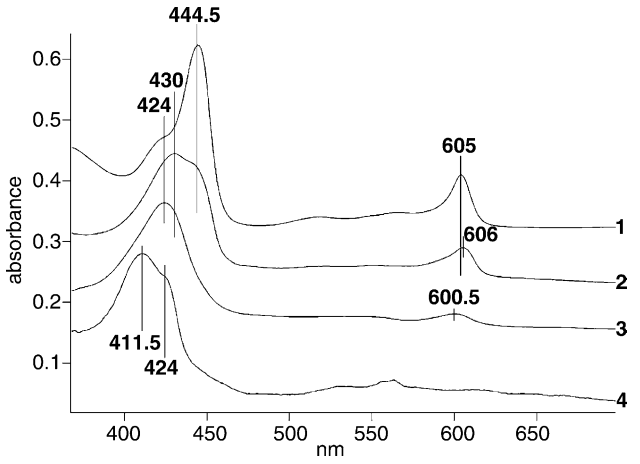

Fig. 1. Low temperature UV–Vis spectra of cytochrome aa_3 and bo_3 oxidase. Spectrum 1: cytochrome aa_3 oxidase fully reduced with ascorbate and PES. Spectrum 2: cytochrome aa_3 oxidase reacted with O_2 for 200 μs. Spectrum 3: fully oxidized cytochrome aa_3 oxidase. Spectrum 4: cytochrome bo_3 oxidase reacted with O_2 for 60 μs. Reference samples for cytochrome bo_3 oxidase are shown in Fig. 18 of [12].

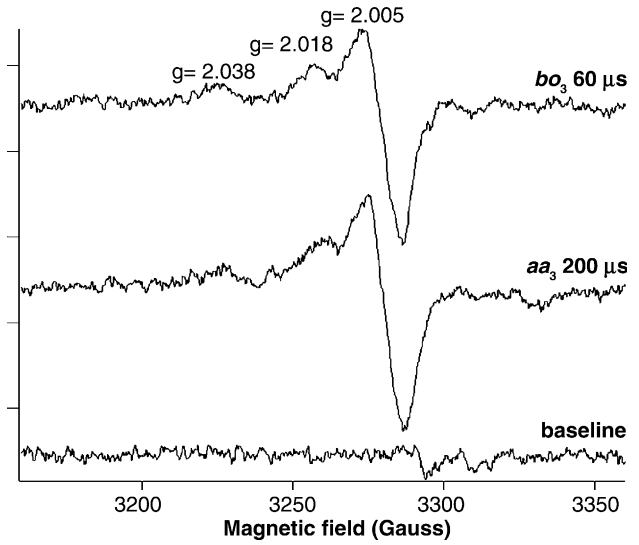

Fig. 2. EPR spectra of transient radicals formed after reaction of cytochrome bo_3 and aa_3 oxidase with oxygen for 60 and 200 μs, respectively. The species with $g = 2.038$, 2.005 is assigned to an oxo-ferryl tryptophan cation radical. The nature of the species contributing to the $g = 2.018$ signal remains to be established. The small negative peaks between 3300 and 3350 G, which do not coincide with those from the baseline, might represent the high field part of a tyrosine radical signal (see text for further explanations). The cytochrome aa_3 spectrum has been corrected for the Mn(II)-signal by subtracting the signal of the fully reduced enzyme. EPR conditions: frequency: 9.25 GHz; microwave power: 200 μW; modulation amplitude: 0.63 mT; temperature: 45 K.

2. Materials and methods

Escherichia coli cytochrome bo_3 oxidase was purified as in [12] and *P. denitrificans* cytochrome aa_3 oxidase as previously described [22]. The MHQ setup is identical to the one described before [12] with the following modifications. Instead of quenching in iso-pentane at 140 K, the sample was sprayed on the inner surface of an aluminum cylinder (height 70 mm, diameter 130 mm, thickness 15 mm), pre-cooled to 77 K and rotating at 7000 rpm. In this way, the surface of the cylinder is covered with a thin layer of sample, optimizing the quenching process. The enzyme reaction temperature is 10 °C.

Samples of 0.5 ml were prepared in anaerobic HPLC vials containing 140 μM cytochrome aa_3 oxidase in 50 mM HEPES buffer, pH 7.2, with 0.05% lauryl-maltoside (LM) or 150 μM of cytochrome bo_3 oxidase in 50 mM K-phosphate buffer, pH 7.5, with 0.05% LM and were reduced with 10 mM ascorbate and 1 μM phenazine ethosulfate (PES). The degree of reduction was followed in situ with a HP 8453 UV–Vis spectrophotometer. The samples were loaded in the injector by means of an O_2-free gastight Hamilton syringe and mixed versus buffer flushed for 30 min with 100% O_2. After the freeze quenching, the Al cylinder was filled with liquid nitrogen and the sample was scraped from the cylinder wall. The frozen powder was collected in a 50 ml Greiner tube first and then used for preparing UV–Vis and EPR samples.

Absorbance spectra were recorded with a SLM-Aminco DW2000 scanning spectrophotometer equipped with a low temperature setup. Part of the quenched sample was transferred into 2 ml cold 140 K iso-pentane and mixed well. Subsequently, a 1-ml aliquot of the sample suspension in iso-pentane was quickly transferred into a pre-cooled sample compartment (light path 2 mm) and frozen in liquid nitrogen. The reference compartment contained iso-pentane. The sample was measured in split-beam mode at a scan-rate of 0.5 nm/s. The spectra shown in Fig. 1 are averages of at least 20 spectra. The averaged spectra were baseline corrected and normalized for the total area of the γ-band to correct for differences in sample amounts. The areas between 400 and 467 nm for the oxidized sample and between 375 and 464 nm for the reduced sample were used for normalization. For samples in different redox states the same area was assumed, which was obtained by small adjustments of the boundaries. EPR spectra were recorded as in [23].

3. Results and discussion

Fig. 1 shows low temperature UV–Vis spectra of cytochrome aa_3 and bo_3 oxidase samples freeze-quenched on the microsecond timescale after direct reaction with molecular oxygen. The absorbance of the 200-μs sample of cytochrome aa_3 oxidase at 444.5 and 605 nm (spectrum 2) is lower by approximately 40% and 20%, respectively, with respect to the fully reduced enzyme (spectrum 1). The new peak at 430 nm, which emerges concomitantly with the disappearance of the absorbance at 444.5 nm, represents the oxo-ferryl form of heme a_3 [10,15,24,25]. Since heme *a* remains largely reduced in the first 200 μs, the enzyme is in the P_M state as is also seen from the small shift to 606 nm in the α-band.

The oxidation kinetics of cytochrome bo_3 oxidase employing MHQ have been reported recently, where the earliest data point was taken after 137 μs (see trace 2, Fig. 18 in [12]). The low temperature UV–Vis spectrum of cytochrome bo_3 oxidase freeze-quenched after 60 μs is shown in Fig. 1. Comparing the two spectra reveals very little differences: similar to the 137-μs sample, heme *b* remains fully reduced in the 60-μs sample, whereas heme o_3 is fully converted to the oxo-ferryl state, Fe^{IV}=O, absorbing at 411.5 nm. From this one can conclude that the enzyme has been converted to the P_M state after reacting for 60 μs with oxygen.

In Fig. 2, EPR spectra in the $g = 2$ region of cytochrome bo_3 (60 μs) and aa_3 (200 μs) oxidase are compared. The spectra show in both cases similar resonances at $g_{eff} = 2.005$ (derivative-like), 2.018 and 2.038 (both absorption-like). The pair of resonances which yield an axial signal with $g_{eff} = 2.038$ and 2.005 is very similar to that detected, e.g., in compound I of cytochrome *c* peroxidase CcPO [26–29] and in compound I of a Phe-Trp-221 mutant of horseradish peroxidase (HRP) [30]. Whereas an isolated radical in X-band EPR yields an isotropic signal at $g \sim 2.005$, we propose that in analogy to compound I,

the axial signal in the oxidases with $g_{x,y} = 2.038$ and $g_z = 2.005$ derives from a weakly exchanged-coupled oxo-ferryl tryptophan cation radical pair. The strength of the exchange coupling between the tryptophan radical ($S = 1/2$) and the heme Fe^{IV}=O system ($S = 1$) can be calculated directly from the observed g-values and from the spin Hamiltonian parameters of the oxo-ferryl system [27–29]. In general, the stronger the interaction, the larger the difference between $g_{x,y}$ and g_z. For the heme a_3 oxo-ferryl tryptophan cation radical with $g_{x,y} = 2.038$, the axial exchange interaction equals $J_{x,y} = -4.9$ GHz.

The origin of the absorption-like resonance at $g = 2.018$ is less clear. It could also be ascribed to a tryptophan radical in interaction with the Fe^{IV}=O state of heme a_3. In that case, the radical with $g_{x,y} = 2.018$ and $g_z = 2.005$ is calculated to have a smaller exchange coupling, $J_{x,y} = -2.1$ GHz. Alternatively, the resonance at $g = 2.018$ might represent the high field part of a tyrosine radical, the central, derivative-like part of such a signal being obscured by the $g = 2.005$ peak; the negative absorption-like peaks to the right of the $g = 2.005$ peak might represent the low field part of a tyrosine radical spectrum (Fig. 2). It should be noted that such an overall spectral width, while quite large for a tyrosine radical (ca. 50 G), is similar to that observed in [17]. Given the uncertainties regarding the $g = 2.018$ signal and the magnetic interaction between the tryptophan radical and the heme a_3 Fe^{IV}=O state, the current best estimate of the total radical concentration amounts to 10–40% of the oxidase concentration in samples yielding the highest EPR radical intensity.

In terms of EPR lineshape and temperature behavior, the signal with $g_{x,y} = 2.038$ and $g_z = 2.005$ in the two oxidases is very similar to that of the oxo-ferryl tryptophan cation radical observed in compound I of the HRP Phe-Trp-221 mutant [30]. The EPR spectrum of the oxidases recorded at 7 K (data not shown) is the same as that shown in Fig. 2, provided the spectrum is recorded at non-saturating microwave power. Although at saturating power the lineshape is distorted, no evidence for the presence of a porphyrin radical was found as, e.g., in compound I of CcPO [27–29].

The EPR spectra of the oxo-ferryl tryptophan cation radical and the $g = 2.018$ species formed in the first steps of the catalytic cycle (Fig. 2) are very different from the spectra assigned to tryptophan/porphyrin radicals obtained under pseudo-equilibrium conditions [21]. The role of the latter in catalysis is therefore unclear, in particular regarding the porphyrin radical, which according to resonance Raman spectroscopy is not formed [15].

Heme–copper oxidases contain two conserved tryptophan residues close to heme a_3, W164 and W272 (*P. denitrificans* numbering) [31,32]. It is interesting to note that W164 is located between heme a and heme a_3. Although the data presented here might suggest a direct role for W164 in mediating electron transfer between the two heme centers, the observed radicals are formed under conditions where heme a has remained reduced, while heme a_3 is in the oxo-ferryl form. Therefore, it is more likely that at least one of the observed radicals acts as electron donor providing one of the four electrons needed to cleave the O–O bond as shown in Fig. 3. We propose that the radical with $g = 2.038/2.005$ is the active site Trp residue W272. The $g = 2.018$ species is due to Trp or Tyr. Although the Y280 radical/Cu_B^{2+} couple has been supposed to be EPR silent [21], we cannot rule it out as the species

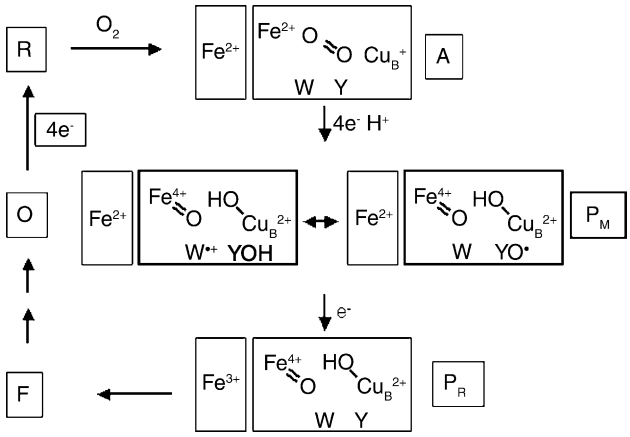

Fig. 3. Proposed reaction scheme for cytochrome oxidase. Modified from [12] and shortened, indicating only the intermediates relevant to this study. The Cu_A site (of cytochrome aa_3) which is in rapid electronic equilibrium with heme a is not depicted; the small rectangle to the left denotes heme a and the large rectangle denotes the binuclear center consisting of heme a_3 and Cu_B. Four electrons and a proton are transferred internally in the transition from A to P_M. Two configurations of the P_M state are shown, which are in rapid electronic equilibrium. One of the four electrons necessary for O–O bond cleavage is delivered either by W272 (shown as W or as $W^{\bullet+}$, the tryptophan cation radical magnetically coupled to the heme a_3 oxo-ferryl) or by the $g = 2.018$ species depicted as X (Trp or Tyr) or in its radical form $X^{\bullet}$; see also text. In the transition from P_M to P_R, an electron is transferred internally from heme a to $W^{\bullet+}$ or $X^{\bullet}$. External electrons delivered from cytochrome c via Cu_A to the heme centers are shown as boxed.

yielding the signal at $g = 2.018$. Our data suggest the formation of radicals on the microsecond timescale in the active site of cytochrome oxidases that are apparently capable of a very fast migration (cf. Fig. 3). Studies are in progress to identify the tryptophan/tyrosine residues involved, to determine the transient kinetics and the protonation state of the radicals and to delineate the redox state of Cu_B in the first steps of the catalytic cycle.

Acknowledgements: This research was financed by the Foundation for Fundamental Research on Matter (FOM Grant D-26), The Netherlands Research Organization (NWO Grant 700-50-025) and the Deutsche Forschungsgemeinschaft (SFB 472). We acknowledge Werner Müller (Frankfurt) for his excellent technical support. We further thank A. van den Berg, R. Suijkerbuijk, J. Langeveld and R. Bode (Delft) for their advice in designing and machining the cold plate setup.

References

[1] Richter, O.M. and Ludwig, B. (2003) Rev. Physiol. Biochem. Pharmacol. 147, 47–74.
[2] Ferguson-Miller, S. and Babcock, G.T. (1996) Chem. Rev. 96, 2889–2908.
[3] Schäfer, G., Engelhard, M. and Müller, V. (1999) Microbiol. Mol. Biol. Rev. 63, 570–620.
[4] Wikström, M.K. (1977) Nature 266, 271–273.
[5] Wang, J., Rumbley, J., Ching, Y.-C., Takahashi, S., Gennis, R.B. and Rousseau, D.L. (1995) Biochemistry 34, 15504–15511.
[6] Babcock, G.T., Jean, J.M., Johnston, L.N., Woodruff, W.H. and Palmer, G. (1985) J. Inorg. Biochem. 23, 243–251.
[7] Pardhasaradhi, K., Ludwig, B. and Hendler, R.W. (1991) Biophys. J. 60, 408–414.
[8] Verkhovsky, M.I., Morgan, J.E. and Wikström, M. (1994) Biochemistry 33, 3079–3086.

[9] Hellwig, P., Grzybek, S., Behr, J., Ludwig, B., Michel, H. and Mäntele, W. (1999) Biochemistry 38, 1685–1694.
[10] Proshlyakov, D.A., Pressler, M.A., DeMaso, C., Leykam, J.F., DeWitt, D.L. and Babcock, G.T. (2000) Science 290, 1588–1591.
[11] Einarsdottir, O. and Szundi, I. (2004) Biochim. Biophys. Acta 1655, 263–273.
[12] Cherepanov, A.V. and De Vries, S. (2004) Biochim. Biophys. Acta 1656, 1–31.
[13] Michel, H. (1999) Nature 402, 602–603.
[14] Babcock, G.T. and Wikström, M. (1992) Nature 356, 301–309.
[15] Ogura, T. and Kitagawa, T. (2004) Biochim. Biophys. Acta 1655, 290–297.
[16] Popovic, D.M. and Stuchebrukhov, A.A. (2004) FEBS Lett. 566, 126–130.
[17] MacMillan, F., Kannt, A., Behr, J., Prisner, T. and Michel, H. (1999) Biochemistry 38, 9179–9184.
[18] Budiman, K., Kannt, A., Luybenova, S., Richter, O.M., Ludwig, B., Michel, H. and MacMillan, F. (2004) Biochemistry (in press).
[19] Svistunenko, D.A., Wilson, M.T. and Cooper, C.E. (2004) Biochim. Biophys. Acta 1655, 372–380.
[20] Fabian, M. and Palmer, G. (1995) Biochemistry 34, 13802–13810.
[21] Rigby, S.E., Jünemann, S., Rich, P.R. and Heathcote, P. (2000) Biochemistry 39, 5921–5928.
[22] Hendler, R.W., Pardhasaradhi, K., Reynafarje, B. and Ludwig, B. (1991) Biophys. J. 60, 415–423.
[23] von Wachenfeldt, C., de Vries, S. and van der Oost, J. (1994) FEBS Lett. 340, 109–113.
[24] Pinakoulaki, E., Pfitzner, U., Ludwig, B. and Varotsis, C. (2003) J. Biol. Chem. 278, 18761–18766.
[25] Kitagawa, T. (2000) J. Inorg. Biochem. 82, 9–18.
[26] Hori, H. and Yonetani, T. (1985) J. Biol. Chem. 260, 349–355.
[27] Houseman, A.L., Doan, P.E., Goodin, D.B. and Hoffman, B.M. (1993) Biochemistry 32, 4430–4443.
[28] Huyett, J.E., Doan, P.E., Gurbiel, R., Houseman, A.L.P., Sivaraja, M., Goodin, D.B. and Hoffman, B.M. (1995) J. Am. Chem. Soc. 117, 9033–9041.
[29] Ivancich, A., Dorlet, P., Goodin, D.B. and Un, S. (2001) J. Am. Chem. Soc. 123, 5050–5058.
[30] Morimoto, A., Tanaka, M., Takahashi, S., Ishimori, K., Hori, H. and Morishima, I. (1998) J. Biol. Chem. 273, 14753–14760.
[31] Ostermeier, C., Harrenga, A., Ermler, U. and Michel, H. (1997) Proc. Natl. Acad. Sci. USA 94, 10547–10553.
[32] Rich, P.R., Rigby, S.E. and Heathcote, P. (2002) Biochim. Biophys. Acta 1554, 137–146.